Eur. Radiol. (2001) 11: 2332–2340
DOI 10.1007/s003300100996

EXPERIMENTAL

BOLD contrast fMRI of whole rodent tumour during air or carbogen breathing using echo-planar imaging at 1.5 T

Willy Landuyt
Robert Hermans
Hilde Bosmans
Stefan Sunaert
Eric Béatse
Davide Farina
Martijn Meijerink
Hao Zhang
Walter Van den Bogaert
Philippe Lambin
Guy Marchal

Received: 6 December 2000
Revised: 26 April 2001
Accepted: 3 May 2001
Published online: 11 July 2001

R. Hermans (✉) · H. Bosmans · S. Sunaert · E. Béatse · D. Farina · M. Meijerink · H. Zhang · G. Marchal
Department of Radiology, KU Leuven, University Hospitals Leuven, 3000 Leuven, Belgium
E-mail: Robert.Hermans@uz.kuleuven.ac.be
Phone: +32-16-343781
Fax: +32-16-343765

W. Landuyt · W. Van den Bogaert · P. Lambin
Laboratory of Experimental Radiobiology and Department of Radiotherapy/Oncology, KU Leuven, University Hospitals Leuven, 3000 Leuven, Belgium

Present address: D. Farina, Cattedra di Radiologia, Università di Brescia, 25123 Brescia, Italy

Present address: P. Lambin, Department of Radiotherapy, RTIL/A. H. Maastricht, Maastricht, The Netherlands

Abstract The aim of this study was to evaluate the feasibility of functional MR imaging (fMRI) at 1.5 T, exploiting blood oxygenation level-dependent (BOLD) contrast, for detecting changes in whole-tumour oxygenation induced by carbogen (5 % CO_2+95 % O_2) inhalation of the host. Adult WAG/Rij rats with rhabdomyosarcomas growing subcutaneously in the lower flank were imaged when tumours reached sizes between 1 and 11 cm^3 (n = 12). Air and carbogen were alternatively supplied at 2 l/min using a snout mask. Imaging was done on a 1.5-T MR scanner using a T2*-weighted gradient-echo, echo-planar imaging (GE-EPI) sequence. Analysis of the whole-tumour EPI images was based on statistical parametric maps. Voxels with and without signal intensity changes (SIC) were recorded. Significance thresholds were set at $p < 0.05$, corrected for multiple comparisons. In continuous air breathing condition, 3 of 12 tumours showed significant negative SIC and 1 tumour had a clear-cut positive SIC. The remaining tumours showed very little or no change. When switching to carbogen breathing, the SIC were significantly positive in 10 of 12 tumours. Negative SIC were present in 4 tumours, of which three were simultaneously characterised by positive SIC. The overall analysis indicated that 6 of the 12 tumours could be considered as strong positive responders to carbogen. Our research demonstrates the applicability of fMRI GE-EPI at 1.5 T to study whole-tumour oxygenation non-invasively. The observed negative SIC during air condition may reflect the presence of transient hypoxia during these measurements. Selection of tumours on the basis of their individual response to carbogen is possible, indicating a role of such non-invasive measurements for using tailor-made treatments.

Keywords Tumour oxygenation · Hypoxia · BOLD fMRI · Carbogen · Radiotherapy · Tumour imaging

Introduction

The inappropriate vascular remodeling and the related hypoxia are critical issues for survival and certainly growth of tumours, as well as for the presence of radio- and chemotherapy resistance; tumours with high oxygenation status on average responded more favourably than those that were poorly oxygenated (e.g. see [1, 2, 3]). This knowledge has led to the introduction and evaluation of agents that may have the potential to promote the oxygenation status of the tumour. Agents such as carbogen (5 % CO_2+95 % O_2) and nicotinamide have been shown to selectively improve tumour oxygenation, both with rodent and human tumours [4, 5, 6]. Subsequently,

the combination of such agents specifically with radiotherapy demonstrated the potential benefit of positive tumour oxygenation changes [7, 8, 9, 10].

Research has in parallel also focused on the measurement of hypoxia levels in tumours, using a battery of different techniques [11, 12, 13, 14, 15]. A drawback is their invasiveness and the absence of whole tumour information. Although improving the understanding of the physiology and biology of different tumour types, such techniques on their own do not meet the requirements to enable, for example, non-invasive repeated oxygenation measurements, before and during treatments, in relatively short time. They also do not allow the assessment of anatomically difficult and deep-seated tumours. The availability of a non-invasive total-body imaging technique could thus positively guide oxygenation modulating treatments that aim to improve tumour control and patient survival.

One potential candidate principle, extensively used in functional MRI (fMRI) to assess brain activity triggered with external stimuli, involves the endogeneous blood oxygenation level-dependent (BOLD) contrast [16, 17, 18]. The BOLD contrast relates to the endogeneous change of paramagnetic deoxyhaemoglobin that is translated in variation of MR signals. The method thus likely offers a non-invasive and clinically applicable tool to detect changes in tumour oxygenation from different treatments without the need to inject contrast agents, nor to disturb the tumour microenvironment. Tumour oxygenation data were collected using fMRI applying a gradient-recalled-echo (GRE) technique, specifically in function of responses to various gas breathing [19, 20, 21, 22]. Two important limitations remain. The measurements were performed with single-slice techniques and they often involved magnetic field strengths above 4 T, except in some limited experience with both animal and patient pilot studies [23, 24, 25, 26]. Extrapolation of these results to lower field strength systems is not straightforward.

The major objective of our investigation was to evaluate the application of BOLD contrast fMRI at a clinical whole body 1.5 T using a fast echo-planar imaging (EPI) sequence, as a non-invasive tool to determine changes in tumour oxygenation from carbogen breathing of the host. The relationship between carbogen responses and tumour volume was also addressed. Finally, the question was raised as to whether the proposed analysis allowed for clear-cut selection of carbogen responsive tumours.

Materials and methods

In vivo tumour model

Male adult WAG/Rij rats, with a body weight of approximately 270 g, were implanted subcutaneously in the lower flank region with a 1-mm^3 piece of syngeneic rhabdomyosarcoma (R1 tumour). At the time of the fMRI study their volume was estimated using a calliper, correcting for the thickness of the skin. The experiments were planned to incorporate various tumour sizes ranging between 0.1 and 14 cm^3.

Animal preparation for imaging

The rats were anaesthetised with 0.1 ml/100 g Nembutal (Sanofi, Brussels, Belgium) injected intraperitoneally a few minutes prior to imaging. To reduce susceptibility artefacts, the animals were placed supine in a flexible plastic recipient, and a mould of approximately 1.5-cm thickness was applied around the tumours and the major part of the body. This mould consisted of the fast setting alginate powder Xantalgin (Bayer Dental, Leverkusen, Germany), remaining flexible and not interfering with the breathing capacity of the animals. It could be removed rapidly from the body without difficulty [27].

Throughout the measurements, the animals were breathing air or carbogen (95 % O_2, 5 % CO_2) at a flow rate of 2 l/min through a small snout mask.

These animal-based experiments were in agreement with the Ethical Committee for Animal Care and Use of the K.U. Leuven (Belgium) and the national guidelines.

Imaging technique

The fMRI studies were performed on a whole-body 1.5-T MR scanner (Magnetom Vision, Siemens, Erlangen, Germany), equipped with a gradient system achieving 25 mT/m in 300 μs. A homemade cylindrical coil of 14 cm diameter was used as antenna.

The imaging sessions consisted of the acquisition of scout images, followed by shimming and fMRI acquisitions. For the fMRI acquisitions, series of sagittal T2*-weighted EPI images were acquired through the entire animal. The parameters for the single shot T2*-weighted EPI sequence used were: TE 39 ms; echo spacing 0.8 ms; bandwidth 1950 Hz/pixel; field of view 288 × 384 mm; matrix 96 × 128; slice thickness 3 mm; and interslice gap 1 mm.

Two series, each consisting of 120 measurements of 16 slices and each lasting 8 min, were obtained sequentially. During the first series air was continuously delivered, whereas during the second series air and carbogen were delivered alternatively (i.e. 1 min of air/5 min of carbogen/2 min of air).

Data analysis

The images were transferred to a workstation (Silicon Graphics), corrected for motion and spatially smoothed by convoluting the data using a Gaussian input function with a full-width at half maximum. Statistical parametric maps (SPM) were computed using SPM96 [28, 29]. The evaluation of the T2*-weighted images was always done with reference to the mean baseline signal intensity (obtained for air condition during the first minute of the imaging) of every individual tumour screening. The different conditions were modeled with a box-car function convolved with the haemodynamic response function implemented as a delayed Gaussian function [30] in the context of the general linear model, as employed by SPM96. Global changes were adjusted for by proportional scaling, and low-frequency confounding effects were removed by an appropriate high-pass filter. Specific effects were tested by applying appropriate linear contrasts to the parameter estimates for each condition, resulting in a *t* statistic for each voxel.

These statistics constitute an SPM. Significance thresholds were set at $p < 0.05$, corrected for multiple comparisons.

Using a mouse-controlled cursor, the borders of the tumours were manually traced on the T2*-weighed EPI images by the same experienced radiologist (R.H.). The number of voxels within the defined tumour volumes was counted, and a MR determined tumour volume was calculated by multiplying the number of voxels with their dimensions ($3 \times 3 \times 4$ mm). The MR-determined tumour volume was compared with the calliper-method using linear regression.

Voxels showing a statistically significant increase or decrease in signal intensity during air breathing were counted. The relative degree of signal intensity changes (SIC) during air condition, compared with the baseline signal intensity, was calculated for each of the voxels showing changes above the significance threshold. By summing up all the negative SIC and separately all the positive SIC, two areas under the curves (AUCs) were calculated. These AUCs were normalised by dividing them by the total number of voxels within the MR-defined tumour volume.

The same type of analysis was applied for the EPI images obtained during the intermittent carbogen breathing condition. These analyses also were performed for all tumours.

The results obtained during the air or the carbogen breathing condition were compared using a paired non-parametric statistical test (Wilcoxon's signed-rank test); p-values < 0.05 were considered significant.

Results

The comparison of the tumour sizes ($n = 12$), as either obtained from the T2*-weighted images or with the calliper, is shown in Fig. 1. The MR-determined volumes of the 12 rat rhabdomyosarcomas under investigation ranged from 1.62 to 10.37 cm^3. Using the calliper method, the volume of the tumours measured just before the fMRI study ranged from 0.9 to 8.9 cm^3. An optimal linear fit was obtained between both methods of measuring volume by using the following function: MR volume = 0.8451×caliper volume+0.3982 ($R = 0.84$).

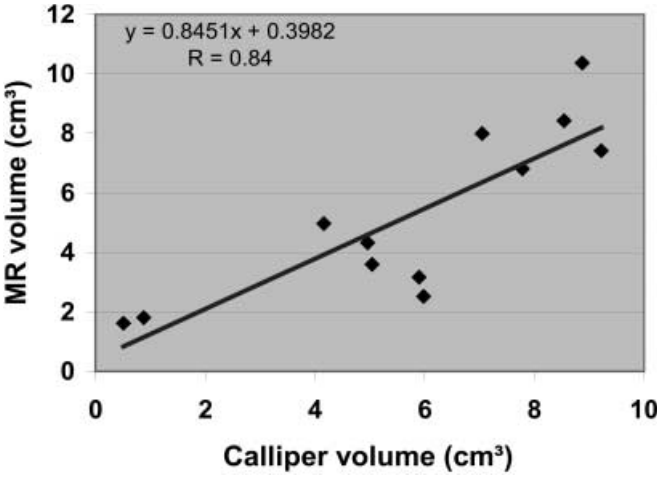

Fig. 1 Comparison of the tumour sizes, determined either with the delineation at the T2*-weighted images (indicated as MR volume) or with the calliper approach

The MR-defined tumour volumes were used throughout the further analysis of all fMRI images. Figure 2 displays a representative image of the rat tumour signal intensity evaluation, both during air breathing (Fig. 2A) and during the carbogen breathing condition (Fig. 2B).

Table 1 gives an overview of the absolute number of voxels that showed positive, negative, or zero signal intensity changes (SIC) either during the continuous air breathing condition or during the switch to carbogen. Figure 3 summarises the voxel-based measurements (percentages deduced from the absolute values presented in Table 1). During the prolonged air breathing, voxels with negative SIC were present in some tumours (Fig. 3A), clearly seen in 6 of the 12 tumours: ≤10 % of the total voxel number in 4 tumours, 27 % and 43 % in 2 other tumours (Table 1). The number of voxels that re-

Table 1 Tumour responses during air or carbogen breathing of the rats; analysis on the basis of voxel numbers (T2*-weighted images)

		Air condition			Carbogen condition		
MR volume (cm^3)	Total number of voxels	Negative	Zero	Positive	Negative	Zero	Positive
1.62	45	0	45	0	1	30	14
1.8	50	0	50	0	11	32	7
2.52	70	0	67	3	1	45	24
3.17	88	9	78	1	2	84	2
3.6	101	11	89	1	12	87	2
4.32	120	51	69	0	2	89	29
4.97	138	37	101	0	0	106	32
6.8	189	0	189	0	42	147	0
7.42	206	0	206	0	0	190	16
7.99	222	16	206	0	1	112	109
8.42	234	5	198	31	0	204	30
10.37	288	17	271	0	5	212	71
	1751	146	1569	36	77	1338	336

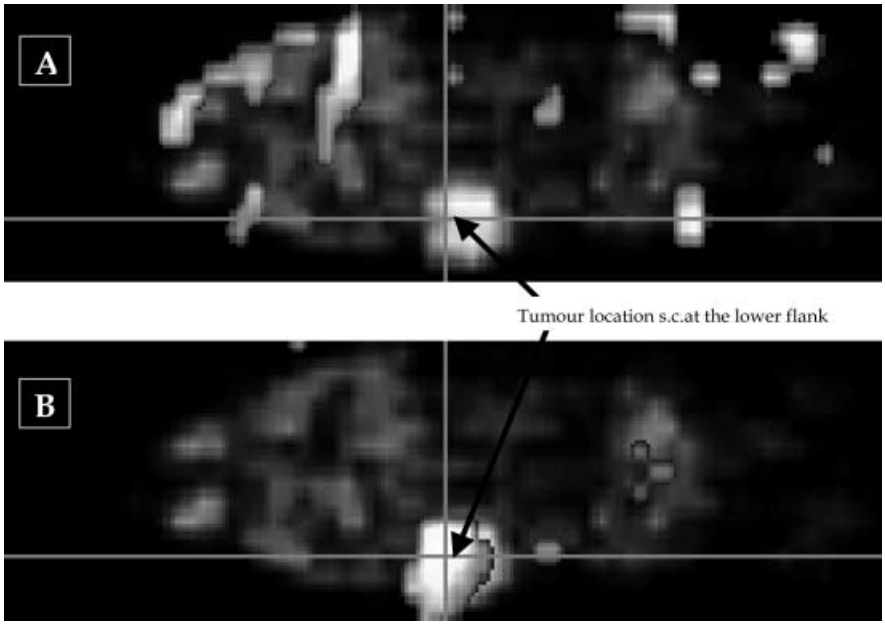

Fig. 2 A, B BOLD fMRI with EPI 39. Example of carbogen-induced (**B**) signal intensity enhancement vs air breathing condition (**A**) within a randomly selected medium-sized rat rhabdomyosarcoma

mained without SIC dominated the picture for the various tumours. In comparison with the results during air breathing, a significantly ($p = 0.022$) lower percentage of voxels showing zero SIC was found during the carbogen breathing (Fig. 3B). This was parallelled by a non-significant ($p = 0.907$) decrease in voxels with negative SIC, and by a highly significant ($p = 0.002$) increase in percentage of voxels with a positive SIC. In 4 tumours for which voxels with negative SIC were recorded during air breathing (< 7 %–43 %), no negative SIC were observed during the carbogen condition (Table 1). A negative change of signal intensity of 22 % and 56 % was observed in 2 tumours, and 5–9 % in 2 others, when the rats breathed carbogen (Table 1). For those tumours that were responsive to carbogen, the change in the EPI T2* signal intensity was very rapid, most often reaching the highest value within 1 min after the switch from air to carbogen (data not shown).

Figure 4 shows the variation in AUC for SIC, present for air breathing and, although to a lesser extent, also for carbogen breathing conditions. No correlation was apparent between the AUC for SIC and the various tumour volumes that were analysed.

Overall, in comparison with the air breathing condition (Fig. 4A), a much larger AUC for the positive signal changes is found during the carbogen breathing

Fig. 3 Box-and-whisker plot for **A** air condition and **B** carbogen condition, representing the percentage of voxels with or without signal intensity changes (SIC), and related to the MR volumes of the tumours investigated. Mean (+) and median *(horizontal bar in the box)*, as well as the 25/75 percentiles *(lower and upper edges of the box)* are indicated. Comparing the carbogen with the air condition, statistical evaluation revealed a highly significant increase in number of voxels with positive SIC ($p = 0.0024$), a lesser but significant ($p = 0.022$) decrease in number of voxels with zero SIC and a non-significant yet clear decrease of the number of voxels with negative SIC

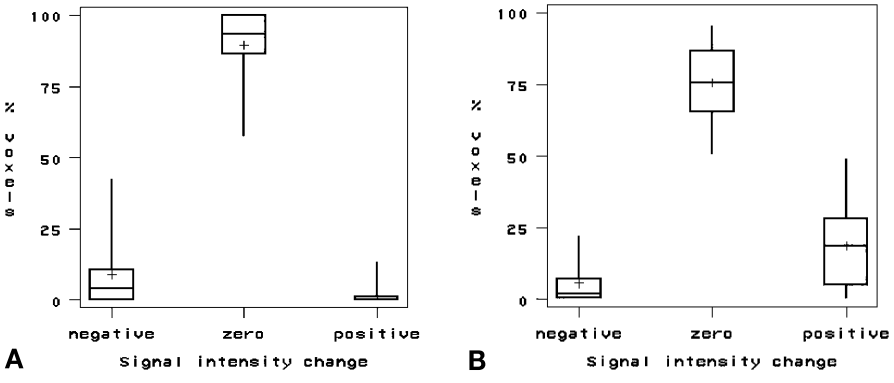

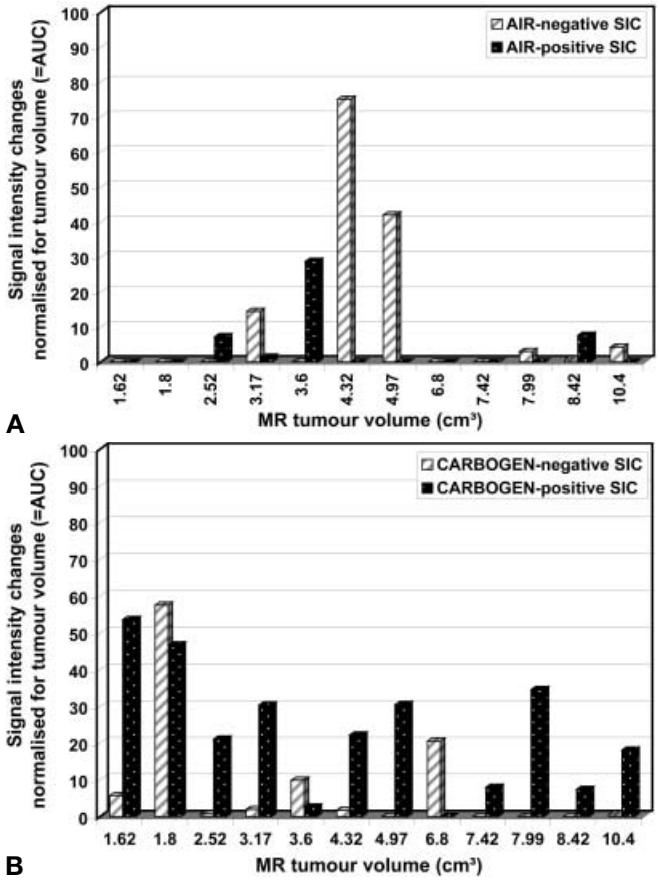

Fig. 4 Display of AUC for the normalized SIC in the responding voxels, for either **A** air or **B** carbogen breathing condition, in relation to the individual MR tumour volumes; *graph A*: the heterogeneous character of the intratumoral SIC during the prolonged air condition, evaluated with respect to the baseline signal intensity (average of first imaging minute), is reflected in positive *(dark bars)* and negative *(clear bars)* SIC; *graph B*: the relative homogeneous positive change in signal intensity *(dark bars)* during carbogen breathing can be deduced for all tumours, except 3 with also or only negative *(clear bars)* SIC. This observation obviously relates to the baseline signal intensity but has increased power when comparison is done with the imaging results for prolonged air condition

(Fig. 4B). As also can be discerned from Fig. 3B, in 3 tumours a clear-cut AUC of negative SIC is present. With these 3 tumours (sizes at imaging = 1.8, 3.6 and 6.8 cm^3, respectively), the benefit of using carbogen to improve the oxygenation status is nil.

Figure 5 displays, only for the carbogen breathing condition, the percentage of voxels showing positive SIC compared with the AUC for degree of positive SIC within the responding voxels for the remaining 9 tumours individually (the main aim of our investigation). The product of the responding voxels and their respective AUC, calculated for each tumour separately, indicates that only 6 of the 12 tumours were very significantly ($p < < 0.05$) responsive to the carbogen application (see Fig. 5 for relative unit for response).

Discussion

In choosing an MR scanning technique for fMRI, spatial resolution, acquisition speed (i.e. temporal resolution) and signal-to-noise ratio (SNR) play an important role. Optimizing one factor will be at the cost of the other two. Echo-planar imaging allows rapid acquisition of a single slice. Repeated measurements of the same slice require a time interval of at least 2 s. In the present study, however, this time window was used for the measurement of adjacent slices. Disadvantages of the technique are the relatively low spatial resolution and the sensitivity to susceptibility artefacts. The large acquisition bandwidth needed for the rapid sampling results in a poor SNR. Susceptibility artefacts are caused by field inhomogeneity at air/tissue interfaces, gradient non-linearity and chemical shift. Using a body-adapted mould, significant improvement of image quality has been obtained by decreasing the magnetic susceptibility at the air/body interface boundary of an animal [27]; however, this correction is not perfect, and may explain the non-optimal correlation ($R = 0.84$) between the tumour volumes determined by the calliper method with those measured on the MRI GE-EPI-images, with the former being the most secure volume approach. The low SNR is compensated by repeated measurements and analysis using statistical methods.

Studies on fMRI of tumours published until now used single-slice GRE sequences at high field strength (e.g. see [19, 20, 21]). The in-plane spatial resolution and SNR during these experiments is better than what can be obtained with the GE-EPI technique that we describe. Applying the GRE technique, however, we could not visualise an effect of carbogen inhalation as attempted in at least 5 tumour-bearing rats, whereas GE-EPI images did show a response in all the tumours that were analysed.

An obvious limitation of GRE images is that the single section may not be representative for the entire tumour. The EPI sequences allow, however, to examine the entire body/tumour in a multi-slice fashion, and may therefore provide a more comprehensive evaluation of the tumour response to carbogen breathing. The limited spatial resolution of GE-EPI introduces a problem of signal averaging within each voxel, and thus a very detailed mapping of tumour oxygenation is not feasible, which counterbalances somewhat the gain of temporal resolution obtainable with this imaging procedure. However, every technique used to estimate tumour oxygenation suffers to some extent from the problem of signal averaging; furthermore, none of the thus far ap-

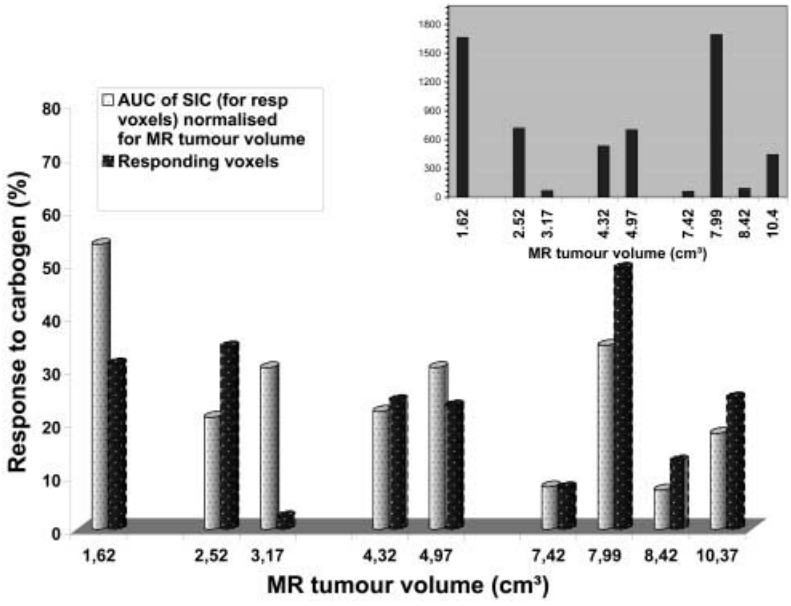

Fig. 5 Overview of the data for only positive intratumoral SIC induced with carbogen breathing of the rats, in relation with tumour size (the three tumours with which strong negative SIC were observed during carbogen, see Fig. 3B, have been omitted). Both, areas under the curves (AUC; *clear bars*) and voxel number *(dark bars)*, are plotted. The "*inset graph*" represents the product of both results of the analysis, and allows to depict the rhabdomyosarcomas that showed a highly significant response (6 of 12 tumours in the present study condition) to carbogen inhalation of the host

plied methodologies, including microelectrode measurements, allows evaluation of the entire tumour.

During the application of the body-adapted mould and the subsequent BOLD contrast fMRI, the animals were immobilised with an anaesthetic. Possible subtle effects of the Nembutal anaesthesia on the effectivity of carbogen breathing and consequently also on the oxygenation of the subcutaneous growing rhabdomyosarcomas cannot be excluded; however, no straightforward agreement on such a bias can be deduced from the literature involving subcutaneous tumour models. Some blood-flow-reducing or hypoxia-inducing effect from this anaesthetic has been reported, but it was insignificant or not at all different from the subcutaneous tumour condition during physical restraint without any sedation [31, 32, 33]. Moreover, all of these published data involved tumours much smaller than 1 cm^3. With our study, the subcutaneous rhabdomyosarcomas were much larger at the time of imaging; thus, inherent to the natural process of hypoxia development during tumour growth, any slight additional hypoxia from the use of the pentobarbital likely will become proportionately of lesser influence anyway. The moulding should not affect the tumour oxygenation condition since it remains flexible, thus allowing the normal breathing of the animals.

The present fMRI data for rat rhabdomyosarcoma show that when carbogen was administered to the rats bearing the rhabdomyosarcoma, a rapid change (< 1 min to reach the maximum) in T2*-weighted signal intensity was observed in most tumours, independent of the tumour size (graphical pixel-by-pixel data analysis not shown). With BOLD contrast GE-EPI fMRI, increases in T2*-weighted signal intensity are related to decreases in deoxyhaemoglobin, and therefore indicative for improved oxygenation in the tissue under investigation. Inversely, decreases in T2*-weighted signal intensity are related to increases in deoxyhaemoglobin and thus likely reflective for tissue hypoxia induction. Other research teams have investigated oxygenation changes under different gas breathing conditions in a variety of tumor systems [19, 20, 21]. The carbogen-induced changes of tumour oxygenation published for these other tumor types with different techniques were, when present, also recorded rapid in time and to a significant extent.

The second observation in our study was the large intertumour variability as well as an important intratumour difference in SIC when the rats breathed carbogen. Separate from the major presence of tumour parts with zero changes, in most tumours positive signal intensity changes were observed (indicating improved oxygenation); however, also negative changes in intensity (indicating reduced oxygenation) were seen both in separate as well as in the same tumours. This was true when analysing both the number of responding voxels and the changes of the signal intensity within these voxels (AUC).

The proportion of voxels with zero SIC (see Table 1) should be interpreted as the simultaneous presence of oxygenated tumour parts and areas of necrosis, proportionately depending on the tumour size at measurement. A correlation between the random distribution/extent of necrosis and the tumour volume in rat rhabdomyosarcomas has been indicated previously by histopathological evaluation of haematoxylin-eosin stained sections of tumours of the present size-range investigated [34]. On the other hand, sufficient haemoglobin saturation with oxygen at the time of imaging could also

explain the absence of a carbogen effect in some tumour parts. This information correlates with the heterogeneous response to carbogen breathing seen in our fMRI studies (present work) and the GRE MRI studies of others (e.g. see [20, 21, 22]). Already in this perspective of heterogeneity, the possibility to analyse the whole tumour in a short time is an attractive and necessary feature to quantitate the variable effects of oxygenation modifying compounds.

The increases in signal intensity observed with MR spectroscopic imaging of subcutaneous R3230AC rat mammary adenocarcinomas (volumes of approximately 0.5 cm^3) have been discussed as the result of improved blood oxygen concentration and oxygen diffusion [35]. Such relationships may likely explain the carbogen-induced positive changes on T2*-weighted BOLD contrast images as measured in the present investigation with subcutaneous rat rhabdomyosarcomas. Also other studies illustrate that the amelioration of tumour oxygenation is highly related to the blood pO_2 increases. With near-infrared spectroscopy, van der Sanden and colleagues demonstrated a clear-cut improvement of the oxyhaemoglobin concentration in tumour blood, when the mice breathed carbogen at any CO_2 content between 1 and 5 % [36]. These measurements were performed on a xenografted human glioma, when tumour size was on average 0.5 cm^3. Obviously, the balance between the rate of oxygen consumption of tumour and stromal cells and the oxygen diffusion during carbogen application will impact on the overall analysis outcome; the latter will therefore and in the first place depend on the tumour type, inplantation site, and its changing general morphology, as well as its quality of vascularity during growth.

Furthermore, and not really surprisingly, carbogen also induced prominent negative signal intensity changes in three rhabdomyosarcomas, independent of tumour size. In at least three studies involving GRE MRI of different tumours, researchers demonstrated a transient decrease in signal intensity or no response during carbogen breathing [21, 23, 37]. Also with MRS, such negative as well as positive SIC from carbogen inhalation compared with air breathing (control condition) have been seen [19]. These observations strengthen the biological reality of this phenomenon. This heterogeneity within a single tumour was attributed by Al Hallaq and colleagues to an intratumoral "steal effect" [19]. They suggested that this could be due to redistribution of blood flow within the tumours. In a patient study, the steal effect seemed the most obvious explanation for the reduced GRE MRI signal during the carbogen breathing as observed in two different tumour types [23]. In our opinion, it could be the result of the intratumoral change in balance between the vasodilating effect from the CO_2 partner and the vasoconstriction effect from the O_2 partner in the carbogen. It should be noted that the breathing of 100 % oxygen either had no effect on the oxy- to deoxyhaemoglobin ratio, or reduced the oxyhaemoglobin concentration in the tumour blood circulation as the result of vasoconstriction [36, 38]. These seemingly conflicting phenomena may well be the result of a similar physiological response from the intratumoral vasculature, partly controlled to a thus far unknown extent of the microvessel maturity and configuration.

Finally, also with the prolonged air-only condition, heterogeneity was appreciated, with tumours showing some positivity in SIC and others with definite evidence of negative SIC. The presence of voxels with negative signal intensity during 8 min of air breathing (identical box-car function analysis as with the carbogen response analysis), as seen strongly in 3 rhabdomyosarcoma tumours and slightly in 3 others, could indicate the occurrence of areas with acute-type transient tumour hypoxia at the time of the MRI multislice measurements. This type of hypoxia is a relatively well-known physiological behavior that is the result of sequential opening and closure of tumour microregional vessels [39, 40]. These intermittent changes of the oxygenation status in tumours may thus relate to a transient reduction in erythrocyte flux, with subsequently alterations in oxygen diffusion and consumption rate (see for discussion e.g. [41, 42]). The time course of transient changes in blood flow within a rat mammary adenocarcinoma has been documented using Fourier analysis and shown to be much stronger present in the tumour as compared with muscle [43].

The overall picture indicates the appropriateness of imaging the whole tumour for the translation of oxygenation changes. Other methods appreciated until now as "standard" (such as Eppendorf pO_2 microelectrode or biopsy-related hypoxia immunohistochemistry) enable a certain yet limited level of knowledge about the oxygenation condition in tumours, and only, however, for those that can be reached. The fMRI data obtained with GE-EPI and presented herein, being non-invasive and short in time, should permit the study of tumour oxygenation also during the treatment phase. Several recent small-scale clinical studies, using either microelectrode pO_2 measurements or perfusion MRI, reported the importance of evaluating tumour characteristics before and during the course of radiochemo- or radiation-only therapy (e.g. [44, 45, 46]).

Our initial results with the rat rhabdomyosarcoma tumour model provide good evidence for the feasibility to image tumour oxygenation using the BOLD fMRI with GE-EPI operating at 1.5 T. Significant inter- and intratumoral heterogeneity in changes in T2*, reflecting changes in intratumoral oxygenation status from the carbogen breathing, were observed. The imaging and analysis methodology enabled the selection of tumours that reacted favourably (or the opposite) to the carbo-

gen breathing of the hosts. The fMRI methodology also allowed to indicate the spontaneous presence of transient hypoxia, as evidenced by the analysis of intratumoral signal intensity fluctuations that occurred during continuous (8 min) air breathing of the rats. The proposed total-body fMRI methodology involving a clinically applicable magnetic field strength and fast whole-tumour screening should help in the selection of differential oxygen-improvement-related treatments.

Acknowledgements We very much appreciated discussions with P. Vanhecke (NMRS Research Unit, K.U. Leuven) and Y. Ni (Experimental Radiology, K.U. Leuven) in various parts of the investigations. Research was partly supported by grants from the Fund for Scientific Research – Flanders and the K.U. Leuven Onderzoeksfonds. R. Hermans is recipient of a EAR-ECR fellowship grant from the ECR 2000 Research and Education Fund.

References

1. Brizel DM, Dodge RK, Clough RW, Dewhirst MW (1999) Oxygenation of head and neck cancer: changes during radiotherapy and impact on treatment outcome. Radiother Oncol 53: 113–117
2. Höckel M, Schlenger K, Mitze M, Schäffer U, Vaupel P (1996) Hypoxia and radiation response in human tumors. Semin Radiat Oncol 6: 3–9
3. Nordsmark M, Overgaard J (2000) A confirmatory prognostic study on oxygenation status and loco-regional control in advanced head and neck squamous cell carcinoma treated by radiation therapy. Radiother Oncol 57: 39–43
4. Bussink J, Kaanders JHAM, Rijken PFJW, Peters JP, Hodgkiss RJ, Marres HA, van der Kogel AJ (1999) Vascular architecture and microenvironmental parameters in human squamous cell carcinoma xenografts: effects of carbogen and nicotinamide. Radiother Oncol 50: 173–184
5. Martin L, Lartigau E, Weeger P, Lambin P, Le Ridant AM, Lusinchi A, Wibault P, Eschwege F, Luboinski B, Guichard M (1993) Changes in the oxygenation of head and neck tumors during carbogen breathing. Radiother Oncol 27: 123–130
6. Powell ME, Collingridge DR, Saunders MI, Hoskin PJ, Hill SA, Chaplin DJ (1999) Improvement in human tumour oxygenation with carbogen of varying carbon dioxide concentrations. Radiother Oncol 50: 167–171
7. Denekamp J, Fowler JF (1997) ARCON–current status: summary of a workshop on preclinical and clinical studies. Acta Oncol 36: 517–525
8. Kaanders JH, Pop LA, Marres HA, Liefers J, van den Hoogen FJ, van Daal WA, van der Kogel AJ (1998) Accelerated radiotherapy with carbogen and nicotinamide (ARCON) for laryngeal cancer. Radiother Oncol 48: 115–122
9. Hoskin PJ, Saunders MI, Dische S (1999) Hypoxic radiosensitizers in radical radiotherapy for patients with bladder carcinoma: hyperbaric oxygen, misonidazole, and accelerated radiotherapy, carbogen and nicotinamide. Cancer 86: 1322–1328
10. Rojas A, Hirst VK, Calvert AS, Johns H (1996) Carbogen and nicotinamide as radiosensitizers in a murine mammary carcinoma using conventional and accelerated radiotherapy. Int J Radiat Oncol Biol Phys 34: 357–365
11. Helmlinger G, Yuan F, Dellian M, Jain RK (1997) Interstitial pH and pO_2 gradients in solid tumors in vivo: high-resolution measurements reveal a lack of correlation. Nature Med 3: 177–182
12. Höckel M, Knoop C, Schlenger K, Vorndran B, Baussmann E, Mitze M, Knapstein PG, Vaupel P (1993) Intratumoral pO_2 predicts survival in advanced cancer of the uterine cervix. Radiother Oncol 26: 45–50
13. Koch CJ, Evans SM, Lord EM (1995) Oxygen dependence of cellular uptake of EF5 [2-(2-nitro-1H-imidazol-1-yl)-N-(2,2,3,3,3-pentafluoropropyl)a cet amide]: analysis of drug adducts by fluorescent antibodies vs bound radioactivity. Br J Cancer 72: 869–874
14. Wijffels KI, Kaanders JH, Rijken PF, Bussink J, van der Hoogen FJ, Marres HA, de Wilde PC, Raleigh JA, van der Kogel AJ (2000) Vascular architecture and hypoxic profiles in human head and neck squamous cell carcinoma. Br J Cancer 83: 674–683
15. Hodgkiss RJ, Jones G, Long A, Parrick J, Smith KA, Stratford MRL, Wilson GD (1991) Flow cytometric evaluation of hypoxic cells in solid experimental tumors using fluorescence immunodetection. Br J Cancer 63: 119–125
16. Ogawa S, LeeTM, Nayak AS, Glynn P (1990) Oxygenation-sensitive contrast in magnetic resonance image of rodent brain at high magnetic fields. Magn Reson Med 14: 68–78
17. Van Zijl PCM, Eleff SM, Ulatowski JA, Oja JME, Ulug AM, Traystman RJ, Kauppinen RA (1998) Quantitative assessment of blood flow, blood volume and blood oxygenation effects in functional magnetic resonance imaging. Nature Med 4: 159–167
18. Kwong KK, Belliveau JW, Chesler DA, Goldberg IE, Weisskoff RM, Poncelet BP, Kennedy DN, Hoppel BE, Cohen MS, Turner R, Cheng HM, Brady TJ, Rosen BR (1992) Dynamic magnetic resonance imaging of human brain activity during primary sensory stimulation. Proc Natl Acad Sci USA 89: 5675–5679
19. Al-Hallaq HA, River JN, Zamora M, Oikawa H, Karczmar GS (1998) Correlation of magnetic resonance and oxygen microelectrode measurements of carbogen-induced changes in tumor oxygenation. Int J Radiat Oncol Biol Phys 41: 151–159
20. Robinson SP, Howe FA, Griffiths JR (1995) Noninvasive monitoring of carbogen-induced changes in tumor blood flow and oxygenation by functional magnetic resonance imaging. Int J Radiat Oncol Biol Phys 33: 855–859
21. Robinson SP, Rodrigues LM, Ojugo AS, McSheehy PM, Howe FA, Griffiths JR (1997) The response to carbogen breathing in experimental tumour models monitored by gradient-recalled echo magnetic resonance imaging. Br J Cancer 75: 1000–1006
22. Howe FA, Robinson SP, Griffiths JR (1996) Modification of tumour perfusion and oxygenation monitored by gradient recalled echo MRI and 31P MRS. NMR Biomed 9: 208–216
23. Griffiths JR, Taylor NJ, Howe FA, Saunders MI, Robinson SP, Hoskin PJ, Powell ME, Thoumine M, Caine LA, Baddeley H (1997) The response of human tumors to carbogen breathing, monitored by gradient-recalled echo magnetic resonance imaging. Int J Radiat Oncol Biol Phys 39: 697–701

24. Lemieux SK, Dorie MJ, Glover GH, Moseley MM, Brown JM, Spielman DM (1995) Tumor response to changes of breathing gas mapped by the functional magnetic resonance imaging technique. Proc ISMRM 2: 898 (abstract)
25. Peller M, Weissfloch L, Shehling MK, Weber J, Bruening R, Senekowitsch-Schmidtke R, Molls M, Reiser M (1998) Oxygen-induced MR signal changes in murine tumors. Magn Reson Imaging 16: 799–809
26. Rijpkema M, Kaanders J, Joosten F, van der Sanden B, Van der Kogel A, Heerschap A (2000) Method to investigate heterogeneity in human tumors by mapping of T2* and gadolinium uptake. ISMRM Workshop, Geiranger, Norway (abstract p 52)
27. Bosmans H, Landuyt W, Farina D, Sunaert S, Béatse E, Hermans R, Lambin P, Marchal G (2000) Improvement of (in vivo) gradient echo imaging using a body-adapted mould: a practical approach. Eur Radiol 10(Suppl 1):425
28. Friston KJ, Jezzard P, Turner R (1994) Analysis of functional MRI time-series. Hum Brain Map 1: 153–171
29. Friston KJ, Worsley KJ, Frackowiak RSJ, Mazziotta JC, Evans AC (1994) Assessing the significance of focal activations using their spatial extent. Hum Brain Map 1: 214–220
30. Friston KJ, Holmes AP, Poline JB, Grasby PJ, Williams SCR (1995) Analysis of fMRI time-series revisited. Neuroimage 2: 45–53
31. Suit HD, Marshall N, Woerner D (1972) Oxygen, oxygen plus carbon dioxide, and radiation therapy of a mouse mammary carcinoma. Cancer 30: 1154–1158
32. Shibamoto Y, Sasai K, Abe M (1987) The radiation response of SCCVII tumor cells in C3H/He mice varies with the irradiation conditions. Radiat Res 109: 352–354
33. Milross CG, Peters, LJ, Hunter NR, Mason KA, Tucker SL, Milas L (1996) Polarographic pO_2 measurement in mice: effect of tumor type, site of implantation, and anesthesia. Radiat Oncol Invest 4: 108–114
34. Landuyt W, Verdoes O, Darius DO, Drijkoningen M, Nuyts S, Theys J, Stockx L, Wynendaele W, Fowler JF, Maleux G, Van den Bogaert W, Anné J, van Oosterom A, Lambin P (2000) Vascular targeting of solid tumours: a major "inverse" volume-response relationship following combretastatin A-4 phosphate treatment of rat rhabdomyosarcomas. Eur J Cancer 36: 1833–1843
35. Karczmar GS, River JN, Li J, Vijayakumar S, Goldman Z, Lewis MZ (1994) Effects of hyperoxia on T2* and resonance frequency weighted magnetic resonance images of rodent tumours. NMR Biomed 7: 3–11
36. Van der Sanden BP, Heerschap A, Hoofd L, Simonetti AW, Nicolay K, van der Toorn A, Colier WN, van der Kogel AJ (1999) Effect of carbogen breathing on the physiological profile of human glioma xenografts. Magn Reson Med 42: 490–499
37. Kuperman VY, River JN, Lewis MZ, Lubich LM, Karczmar GS (1995) Changes in T2*-weighted images during hyperoxia differentiate tumors from normal tissues. Magn Reson Med 33: 318–325
38. Hill SA, Collingridge DR, Vojnovic B, Chaplin D (1998) Tumour radiosensitization by high-oxygen-content gases: influence of the carbon dioxide content of the inspired gas on pO_2, microcirculatory function and radiosensitivity. Int J Radiat Oncol Biol Phys 40: 943–951
39. Reinhold HS, Blackiwiecz B, Blok A (1977) Oxygenation and reoxygenation in "sandwich" tumors. Bibl Anat 15: 270–272
40. Chaplin DJ, Olive PL, Durand RF (1987) Intermittent blood flow in a murine tumour: radiobiological effects. Cancer Res 47: 597–601
41. Chaplin DJ, Hill SA (1995) Temporal heterogeneity in microregional erythrocyte flux in experimental solid tumours. Br J Cancer 71: 1210–1213
42. Trotter MJ, Chaplin DJ, Olive PL (1991) Possible mechanisms for intermittent blood flow in the murine SCCVII carcinoma. Int J Radiat Biol 60: 139–146
43. Braun RD, Lanzen JL, Dewhirst MW (1999) Fourier analysis of fluctuations of oxygen tension and blood flow in R3230Ac tumors and muscle in rats. Am J Physiol 277:H551–H568
44. Stadler P, Feldmann HJ, Creighton C, Kau R, Molls M (1998) Changes in tumor oxygenation during combined treatment with split-course radiotherapy and chemotherapy in patients with head and neck cancer. Radiother Oncol 48: 157–164
45. Mayr NA, Yuh WT, Magnotta VA, Ehrhardt JC, Wheeler JA, Sorosky JI, Davis CS, Wen BC, Martin DD, Pelsang RE, Buller RE, Oberley LW, Mellenberg DE, Hussey DH (1996) Tumor perfusion studies using fast magnetic resonance imaging technique in advanced cervical cancer: a new noninvasive predictive assay. Int J Radiat Oncol Biol Phys 36: 623–633
46. Knopp MV, Lumer MM, Schlemmer HPW, Dietz A, Lucht R, Hawighorst H, Vanselow B, van Kaick G (2000) Functional MRI of head and neck carcinomas to assess microcirculation and changes during therapy. Eur Radiol 10 (Suppl 1):111